BIOCHEMISTRY
including biophysical chemistry & molecular biology

Article

pubs.acs.org/biochemistry

Bifurcation in the Ultrafast Dynamics of the Photoactive Yellow Proteins from *Leptospira biflexa* and *Halorhodospira halophila*

L. Tyler Mix,[†] Julia Kirpich,[†] Masato Kumauchi,[‡] Jie Ren,[‡] Mikas Vengris,[§] Wouter D. Hoff,[‡] and Delmar S. Larsen*[,†]

[†]Department of Chemistry, University of California, Davis, One Shields Avenue, Davis, California 95616, United States
[‡]Department of Microbiology and Molecular Genetics, Oklahoma State University, Stillwater, Oklahoma 74078, United States
[§]Faculty of Physics, Laser Research Centre, Vilnius University, Sauletekio 10, LT-10233 Vilnius, Lithuania

Supporting Information

ABSTRACT: We explored the photoisomerization mechanisms in novel homologues of photoactive yellow protein (PYP) from *Leptospira biflexa* (Lbif) to identify conserved features and functional diversity in the primary photochemistry of this family of photoreceptors. In close agreement with the prototypical PYP from *Halorhodospira halophila* (Hhal), we observe excited-state absorbance near 375 nm and stimulated emission near 500 nm, with triphasic excited-state decay. While the excited-state decay for Lbif PYP is the slowest among those of known PYPs due to the redistribution of the amplitudes of the three decay components, the quantum yield for productive photocycle entry is very similar to that of Hhal PYP. Pro68 is highly conserved in PYPs and is important for the high photochemical quantum yield in Hhal PYP, but this residue is Ile in wild-type Lbif PYP. The level of photoproduct formation is slightly increased in I68P Lbif PYP, indicating that this residue regulates the photochemical quantum yield in the entire PYP family. Lbif PYP also exhibited a blue-shifted photoproduct previously undiscovered in ultrafast studies of PYP, which we have named pUV. We posit that pUV is a detour in the PYP photocycle with a twisted protonated *p*CAH configuration. Cryokinetic experiments with Hhal PYP confirmed the presence of pUV, but the population of this state in room-temperature ultrafast experiments is very small. These results resolve the long-standing inconsistency in the literature regarding the existence of a bifurcation in the room-temperature photocycle of PYP.

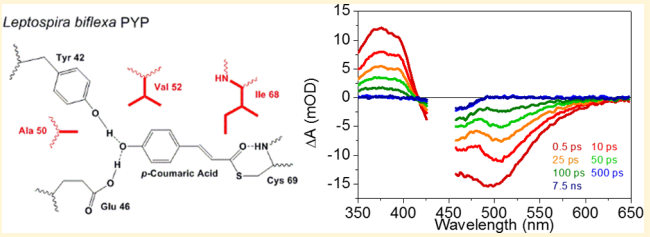

Sunlight provides the energy necessary to support life in the Earth's biosphere. Sunlight is responsible for driving photosynthesis processes and modulates a wide range of other important light-driven bioactivities, including phototaxis,[1,2] gene expression,[3] and vision.[4,5] Moreover, photobiological processes are responsible for the mechanisms that modulate the expression of photosynthetic infrastructure via complementary chromatic adaptation.[6] The transduction of light energy into usable function is performed by two distinct processes to accomplish transmembrane proton transfer in membrane proteins. The first process proceeds via electron transfer in chlorophyll-based photosynthetic reaction centers.[7] The second process is driven by double-bond photoisomerization in the chromophore of retinal-based proteorhodopsins.[8] The photochemical fate of the electronically excited state formed upon light absorption is different in these two classes of photoactive proteins. While the parameters that govern electron transfer are well understood,[9] the factors that control chromophore photoisomerization to initiate the signaling process have been a topic of active interest. Proteins that use light energy to initiate biological signaling are termed photoreceptors, and this process is often initiated by chromophore photoisomerization.

The chromophore binding pocket of photoreceptor proteins often greatly increases the quantum yield and specificity for the alkene photoreceptor compared to those of the free chromophore in solution,[10,11] while reducing fluorescence quantum yields. This issue is of primary importance for bioenergetics, biological light sensing, and the use of photoreceptors as light-activated switches in the emerging field of optogenetics.[12] Optogenetics, using light to control biological processes, depends on having access to well-understood photoreceptors.[13] We are studying the influence of the chromophore binding pocket on photoreceptor yield and dynamics using the photoactive yellow protein (PYP) as a model system. PYP is a small, 14 kDa, 125-residue, water-soluble protein with complex photochemistry that is initiated by the photoexcitation of an embedded *p*-coumaric acid (*p*CA) chromophore covalently attached to Cys69 (Scheme 1).[14] In the dark-adapted pG state, the *p*CA is deprotonated with the double bond in its coumaryl tail in the *trans* configuration. Upon the absorption of a blue photon, an excited-state

Received: May 30, 2016
Revised: October 13, 2016

DOI: 10.1021/acs.biochem.6b00547
Biochemistry XXXX, XXX, XXX−XXX

Scheme 1. Local Protein Environment around the *p*CA Chromophore for Hhal PYP (left) and Lbif PYP (right)[a]

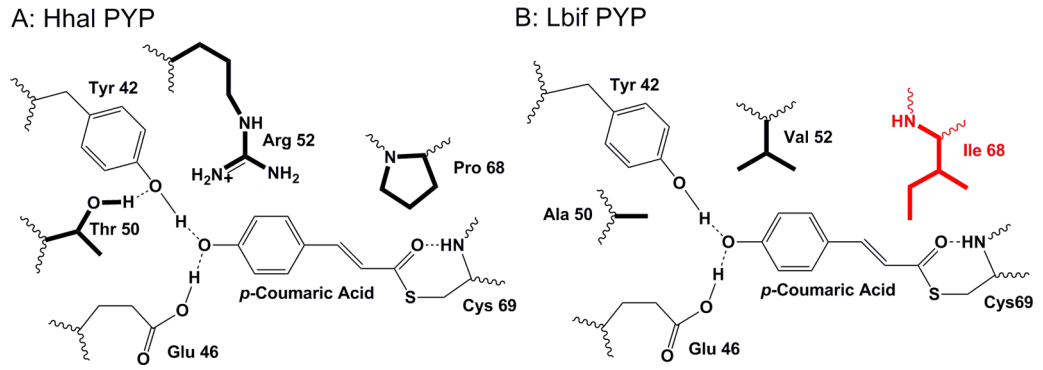

[a]The residues shown in bold are different between the proteins, and the Ile68 residue (red) is modified to a Pro residue in the mutant Ile68Pro Lbif PYP.

isomerization reaction occurs that generates a *cis* conformation on a picosecond time scale.[15,16] This triggers several ground-state steps, including an intramolecular proton transfer to the phenolic end of the chromophore and then large-scale structural changes in the protein through the alterations of hydrogen bonding interactions.[17−19] The diversity of chemical reactions in PYP makes it a rich system for investigating how a protein structure and dynamics guide chromophore dynamics and vice versa.

The vast majority of studies aimed at understanding the photoactivity of PYP have focused on the protein isolated from the proteobacterium *Halorhodospira halophila* (Hhal PYP),[20] including mutants[21−25] or Hhal PYPs expressed with modified chromophores.[26] While close to 100 PYP homologues have been identified in genomes, few studies have been reported on the photochemical characterization of PYPs from these other organisms.[27,28] Recently, we identified a PYP homologue in the spirochete *Leptospira biflexa* (Lbif PYP) with an amino acid sequence that is only 38% identical and 56% similar to that of Hhal PYP.[27] The *p*CA chromophore pockets of Hhal PYP and Lbif PYP are qualitatively similar (Scheme 1) with three key differences. (i) Residue 68, which is immediately adjacent to Cys69, is an isoleucine in Lbif PYP but a proline in >90% of all PYPs identified to date.[27] (ii) Residue 52 at the interface between *p*CA and the solvent is an arginine in Hhal PYP but a nonpolar valine in Lbif PYP. (iii) Residue 50 is a threonine in Hhal and an alanine in Lbif PYP.

In Hhal PYP, the Thr50 residue contributes to the hydrogen bonding network between *p*CA and the surrounding protein scaffolding, while the Ala50 residue in Lbif PYP does not participate in the hydrogen bonding network. The hydrogen bonding network is integral in the formation of the light-adapted pB state.[11] Substitutions at position 50 induces substantial red shifts in the absorbance spectrum of the protein in Hhal PYP,[11,28,29] and this is presumably the origin of the red-shifted spectrum in Lbif PYP (Figure 1).

The role of Arg52 in the Hhal PYP photocycle is disputed as experiments with the Arg52Gln mutant showed a slight decrease in the speed of the reaction, but the mutant retained photoproduct production similar to that of WT Hhal PYP.[22] However, molecular dynamics simulations by Groenhof et al. indicate that a positively charged Arg52 controls which of the bonds isomerizes in the *p*CA chromophore,[30] while the mutant with Gln52 isomerized at the nearby single bond (C_3−C_1).[31] Further experiments have argued that Arg52 in PYP is not

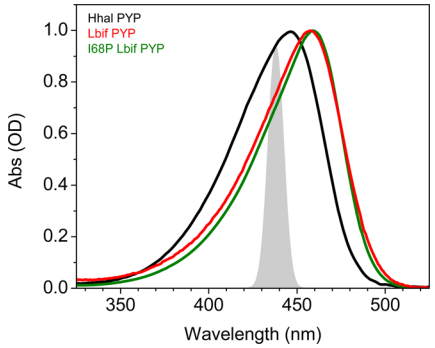

Figure 1. Steady-state normalized absorption spectra of Hhal PYP (black), Lbif PYP (red), and I68P mutant Lbif PYP (green) in the pG state with *p*CA in the *trans* conformation (Scheme 1). The laser spectrum of the 438 nm excitation pulses (gray) is indicated.

charged[32] and may not influence the forward isomerization reaction for the Arg52Ala mutant.[33] Because the photocycle proceeds with the Arg52Gln[22] and Arg52Ala[33] mutations, it is believed that the carbonyl flip and breaking the hydrogen bond with the amine backbone of Cys69 are the crucial actions in the initial photoreaction.[17,31]

A suggested role of Pro68 in WT Hhal PYP was that this residue constrict the chromophore pocket, leading to isomerization. When residues with smaller side chains are mutated into position 68,[21,34] the photoreaction is slowed considerably. Groot et al. also reported that smaller residues have a more pronounced effect in decreasing the quantum yield in initiating the photocycle.[21]

While extensive studies have yielded a deep and detailed understanding of the molecular mechanisms of the initial steps of the PYP photocycle,[15,17,35,36] important unresolved issues remain. First, the decay of the electronically excited state is triphasic, but the underlying quenching mechanisms are unclear. Second, the role of the residues surrounding the chromophore pocket and the influence of the apoprotein in non-Hhal PYP systems have not been explored. Third, Imamoto and co-workers reported evidence of cryogenic measurements for the existence of an early blue-shifted photocycle intermediate (at ∼450 nm), called PYP_H.[37,38] However, most other studies that reported ultrafast visible pump−probe experiments have found no evidence of such an early blue-shifted state.[21−23,36] Here we report data that yield novel insights into all three issues, through ultrafast transient

DOI: 10.1021/acs.biochem.6b00547
Biochemistry XXXX, XXX, XXX−XXX

absorption on the first non-Hhal PYP protein, Lbif PYP, and through low-temperature kinetic different absorption experiments with Hhal PYP.

MATERIALS AND METHODS

Mutant Preparation. The synthetic gene encoding WT Lbif PYP cloned into pUC19 was obtained from Epoch Life Science Inc. This gene was recloned into the PQE-80L vector at the *Bam*HI and *Pst*I sites, and the sequence of the inset was confirmed by an ABI 3730 DNA analyzer at the Oklahoma State University DNA/Protein Core Facility. This plasmid was used as template DNA in a mutagenic polymerase chain reaction (PCR) to introduce the I68P mutation. Mutagenesis was performed using the two-step outlines of Mihara et al.[39] with minor modifications. The first step was to amplify the gene between the primers PQE-FW (flanking sense primer) and mutation-RV (mutation antisense primer) or Lb-RV (flanking antisense primer) and mutation-FW (mutation sense primer). The second step combines the amplified gene products to amplify the entire Lb-PYP mutant gene with *Bam*HI and *Pst*I restriction sites. The PCR product was digested with *Bam*HI and *Pst*I and then ligated into PQE-80L at the same restriction sites, followed by transformation into *Escherichia coli* strain DH-5α. The resulting plasmid DNA confirmed the DNA sequence, as well. DNA primer sequences are available in the Supporting Information.

Protein Expression, Reconstitution, and Purification. The plasmids encoding WT and Ile68Pro mutant Lbif PYPs were transformed into *E. coli* strain BL21(DE3) and used to obtain the corresponding apoPYP samples. The *E. coli* strains were incubated in 1 L of LB medium containing 50 mg/mL ampicillin at 37 °C for 16−18 h and IPTG (isopropyl thio-β-galactoside, final concentration of 1 mM) for inducing protein expression. The cells were harvested 4 h after induction by centrifugation (Sorval, 4000 rpm, 10 min) and disrupted with 8 M urea, and the cell debris was spun down (Beckmann, 20K rpm, 20 min). The supernatant was diluted 2-fold by the addition of buffer [10 mM Tris-HCl (pH 7.5)] under magnetic stirring followed by the addition of 200 μL of *p*-hydroxycinnamic anhydride. The reconstituted holoPYP was dialyzed against Tris-HCl buffer (10 mM, pH 7.5). The dialyzed PYP was applied to Ni-NTA (Qiagen) followed by purification using CM Sepharose (Sigma-Aldrich). The purity of the protein was confirmed by sodium dodecyl sulfate−polyacrylamide gel electrophoresis. The final protein samples used for the ultrafast measurements were in 10 mM Tris-HCl buffer (pH 7.5).

Ultrafast Spectroscopy. The primary light source was an amplified Ti:sapphire laser system (Spectra Physics Spitfire Pro) that delivered 1 kHz pulses at 800 nm with an energy of 2.5 mJ and a 40 fs full width at half-maximum (fwhm) duration. The laser beam was split into two separate pathways for the independent generation of the pump and probe pulses. The 438 nm pump pulses were produced by sum frequency generation of the near-IR output of a home-built noncollinear optical parametric amplifier (NOPA) with 800 nm pulses in a 1 mm thick β-barium borate (BBO) nonlinear crystal (Figure 1, gray curve). Broadband probe pulses were generated by focusing a portion of the fundamental 800 nm pulses (~500 nJ) into a slowly translating 2 mm CaF_2 crystal. After being temporally and spatially overlapped with the pump pulses in the PYP sample, the probe light was detected by an imaging spectrograph (Oriel MS 127i) equipped with a 256-pixel photodiode array (Hamamatsu S3901 and C7884). The pump beam was modulated by a mechanical chopper to 500 Hz to collect difference spectra between the pumped and unpumped samples. The probe pulses were mechanically delayed from −10 ps to 7.5 ns with respect to the pump pulse by a computer-controlled linear motor stage (Newport IMS 600). The polarization of pump and probe pulses was set at 54.7° (magic angle) with respect to each other to eliminate anisotropic effects associated with rotational dynamics. The samples were passed continuously through a commercial quartz 1 mm flow cell (Starna) to provide fresh protein for each laser shot, and the sample was maintained at room temperature during all measurements. The resulting transient absorption (TA) signals had an ~125 fs temporal resolution (instrumental response function), estimated by the rise of the excited-state absorption (ESA) band. The ultrafast broadband TA signals of Lbif PYP, I68P Lbif PYP, and Hhal PYP were measured consecutively on the same experimental setup and under the same experimental conditions to allow direct comparison of the data. The 438 nm excitation wavelength was selected to avoid multiphoton ionization of *p*CA.[36,40] A cartoon of the experimental setup is available in Figure S1.

Cryokinetic Spectroscopy. The low-temperature cryokinetic measurements were performed using an Oxford Instruments Optistat DN liquid nitrogen cryostat placed in the beam path of a Shimadzu UV−vis spectrometer. The PYP sample was dissolved in a solution of 66% glycerol and 33% buffer in a custom designed cell. The cryokinetic measurements were performed in two separate (back-to-back) experiments because of increased light scattering from the sample when the vitrified sample "cracks" at very low temperatures to generate a high-scattering sample: (i) from 160 to 290 K and (ii) from 80 to 160 K. Experiments begin at the highest temperature, 290 or 160 K, and reference spectra are recorded every 3 min for 33 min. Next the temperature is "dropped" by 10 K, to 280 or 150 K. Each temperature drop is completed in <2 min (based on the measured cryostat temperature); however, the sample thermalizes on a slower (8−10 min) time scale where the absorption spectra sharpen and blue-shift. The cooling signals are collected for 33 min to capture the thermal equilibration at every temperature and more importantly to measure a fully equilibrated "reference spectrum" to use with the illuminated cryokinetic spectra discussed below. The temperature drop kinetics and terminal reference spectra are repeated at 10 K until the target temperature (either 160 or 80 K) is reached.

At the target temperature, the sample is illuminated for 30 min with 440 nm light to initiate the photocycle. After illumination, spectra are collected every 3 min for 72 min. The temperature is increased 10 K, to 170 or 90 K, which allows the photocycle to proceed, and sample spectra are collected again for 72 min. Sample spectra are collected at each 10 K upward jump as the cryostat warms until the starting temperature is reached. The differences between the final reference spectra and each illuminated spectra at the same temperature are calculated to eliminate the influence of thermal equilibration and create spectra that resemble ultrafast transient absorption spectra for ease of interpretation. A flowchart depicting the cryokinetic measurement process is available in Scheme S1.

RESULTS

Ultrafast UV−Vis Pump−Probe Experiments. The absorption spectrum of Hhal PYP in the dark-adapted pG-state peaks at 446 nm (Figure 1, black curve), and the pG spectra of wild-type Lbif and Ile68Pro PYPs are red-shifted to

DOI: 10.1021/acs.biochem.6b00547
Biochemistry XXXX, XXX, XXX−XXX

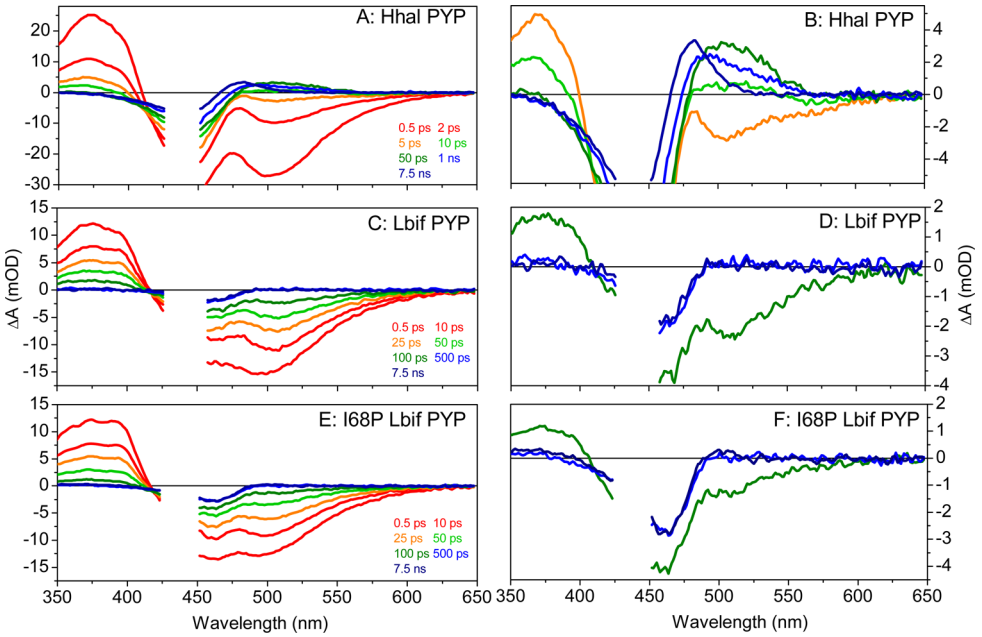

Figure 2. Transient absorption spectra at selected time points for HhaI PYP, Lbif PYP, and Ile68Pro Lbif PYP with expanded views of the later time points in the second column. The sample was excited at 438 nm with 125 nJ. Spectra are color-coded by time for each protein.

Table 1. Global Analysis Parameters Optimized by Target Analysis of the Difference Absorption Spectra for HhaI PYP, Lbif PYP, and Ile68Pro Lbif PYP[a]

	pG* 1	pG* 2	pG* 3	GSI 1	I_0	pR
			HhaI PYP			
population (%)	52	42	6			
lifetime (ps)	0.5	2.7	45	2	1200	∞
branching yields (%)	22 (GSB)					
	14 (GSI)	71 (GSI)	99 (GSI)		36 (GSI)	
	64 (I_0)	29 (I_0)	1 (I_0)		64 (pR)	
pR yield (%)	21	8	0.02			total of 29
			Lbif PYP			
population (%)	23	25	52			
lifetime (ps)	0.2	7	64	not observed	2.4	∞
branching yields (%)		92 (GSB)	99 (GSB)			
	100 (I_0)	8 (I_0)	1 (I_0)		100 (pR)	
pR yield (%)	23	4	0.2			total of 27
			Ile68Pro Lbif PYP			
population (%)	26	24	50			
lifetime (ps)	0.2	9	45	not observed	0.8	∞
branching yields (%)		92 (GSB)	99 (GSB)			
	100 (I_0)	8 (I_0)	1 (I_0)		100 (pR)	
pR yield (%)	26	4	0.2			total of 30

[a]The relative error for each parameter is 10% with the exception of the quantum yields for Lbif PYP and Ile68Pro Lbif PYP, whose relative error approaches 20%.

465 nm (red and green curves, respectively). This can be ascribed to the absence of a hydrogen bond between residue Thr50 and Tyr42 based on the Thr50Ala mutation on the absorption HhaI PYP (Scheme 1).[23] The TA spectra of HhaI PYP, Lbif PYP, and Ile68Pro Lbif PYP at select times are contrasted in Figure 2. For HhaI PYP (Figure 2A), the initial signal amplitude is ∼37 mOD while the noise level is ∼0.1 mOD, yielding a signal-to-noise (S/N) ratio of ∼370. For both Lbif PYP (Figure 2C,E), the total signal amplitude is ∼19 mOD and the noise level is ∼0.1 mOD, yielding a S/N ratio of ∼190.

The initial spectra for both Lbif PYP samples exhibit features similar to those found in HhaI PYP (Figure 2A,C,E) with negative ground-state bleaches (GSBs) at 460 nm for Lbif PYP and 445 nm for HhaI PYP due to loss of pG absorption (Figure 1), a negative band ascribed to stimulated emission (SE) of the excited-state pG* population at 500 nm, and a positive band at 375 nm ascribed to an excited-state absorption (ESA) of pG*. The spectral similarity of these three PYP systems indicates that the differences in the *p*CA chromophore pocket between the samples (Scheme 1) do not alter the basic photophysical

DOI: 10.1021/acs.biochem.6b00547
Biochemistry XXXX, XXX, XXX−XXX

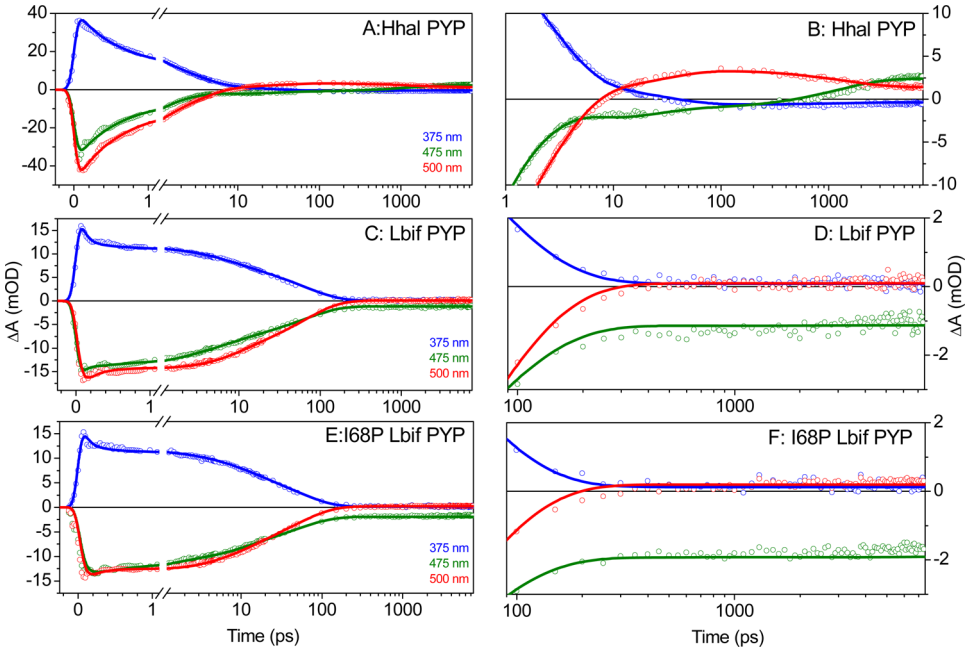

Figure 3. Transient absorption kinetics at select wavelengths for WT Hh PYP, WT Lb PYP, and I68P Lb PYP. A logarithmic scale is used in each trace after 1 ps.

properties of the system and that modeling and interpretations developed for Hhal PYP can be extended to the Lbif PYP samples. As expected for the 438 nm excitation, no ionization features (i.e., solvated electron or *p*CA radical) were observed in any of the measured signals, indicating these are clean single-photon-initiated signals.[36,40]

While the GSB, ESA, and SE bands of pG* are well-resolved for both Hhal and Lbif samples (Figure 2), the subsequent ground-state photointermediate spectra are significantly better resolved for Hhal. The 50 ps spectrum for Hhal PYP (Figure 2B) reveals positive signals ascribed to photoproduct formation in the region of 470−530 nm with properties closely matching previously published results.[21−23,36] This spectrum is characteristic of the primary photoproduct, I_0, that is generated via a high-quantum yield excited-state isomerization reaction [~0.45 (Table 1)].[36,41] Moreover, because I_0 is spectrally red-shifted compared to the negative pG bleach at 445 nm, it is well resolved in Hhal PYP.

The I_0 blue shifts on a 1 ns time scale to generate the pR intermediate at 475 nm.[21−23,36] The kinetic traces for Hhal PYP (Figure 3B) show the conversion of the I_0 state into the pR state as the intensity of the positive signal at 500 nm (red curve) decreases significantly from 100 ps to 7.5 ns, while the intensity of the signal at 475 nm (green curve) increases. No features of the $I_0^{\ddagger}$ intermediate proposed previously[42] between I_0 and pR were resolved in the data (with a 220 ps lifetime), nor from the global analysis of these data (see below). Subsequent evolution of the photocycle[35,43] is beyond the time range of the experiment.

In contrast to the spectral similarities between the pG* spectra of the Hhal and Lbif PYPs (Figure 2), the temporal properties differ significantly among the three samples (Figure 3). In Hhal PYP, the ESA band at 375 nm (blue curve) and the SE band at 500 nm (red curve) have almost fully decayed by 10 ps (Figure 3B). However, in Lbif PYP (Figure 3B,C), these excited-state signals are significantly slower; the kinetic traces in Figure 3 at 375 nm (blue curve) and 500 nm (red curve) show that the ESA and SE bands in Lbif PYP (Figure 3C,E) persist beyond 200 ps.

While all three PYP samples exhibit similar pG* spectra, the resulting photoproduct spectra differ appreciably. In the case of Lbif PYP, the amplitude of the red-shifted photoproduct spectrum is greatly reduced, which is likely caused by the stronger spectral overlap of the photoproduct absorption with the pG GSB. Compared with that of Hhal PYP, the GSB of Lbif PYP is red-shifted by 15 nm to 460 nm (Figure 1) and presumably obscures the photoproduct signal. A weak positive absorption feature is detected on the red side that peaked at 500 nm in the final spectrum at 7.5 ns (Figure 2D,F and Figure S6). The amplitude of this photoproduct band is ~10-fold smaller than that observed for Hhal PYP, which may indicate a lower quantum yield (within the noise level of the measurement) but is more likely caused by the red-shifted Lbif PYP GSB. To explore the molecular basis for the reduced photochemical quantum yield in Lbif PYP, we examined the role of residue 68 (Scheme 1); Pro68 promotes I_0 formation in Hhal PYP,[21] and Lbif PYP is unusual because residue 68 is an isoleucine. The decay kinetics was weakly affected in the Ile68Pro mutant of Lbif PYP (Figure 3E), and the amplitude of the red-shifted photoproduct is higher in Ile68Pro Lbif PYP than in WT Lbif PYP (Figure 2C−F).

Global Analysis. Multicompartment global analysis techniques were used to quantitatively describe the ultrafast signals for the Hhal and Lbif PYP samples.[44,45] In this analysis, we rely on the approaches that were developed for PYP in extensive research.[21,23,36,41] The transient spectra were initially fit with a sequential system of differential equations to produce evolution-associated difference spectra (EADS) and the apparent lifetimes (Figure S1). These spectra do not represent individual populations in PYP but are linear combinations of the true species-associated difference spectra (SADS). To extract the SADS for WT Hhal PYP, a heterogeneous model was based on previous analysis of Hhal PYP (Scheme 2).[21,23,36] In this model, the photoexcitation of three dark-adapted pG

DOI: 10.1021/acs.biochem.6b00547
Biochemistry XXXX, XXX, XXX−XXX

Scheme 2. Target Kinetic Model for HhaI PYP and Adapted to Lbif PYP[a]

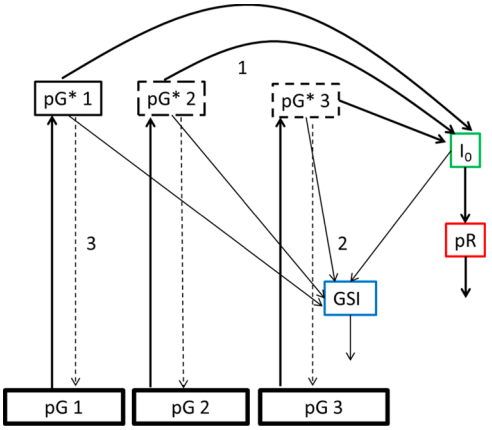

[a]Each pG* may proceed through three possible paths: to photoproducts (1), to the ground state via the GSI state (2), or directly to the ground state (3). In HhaI PYP, the excited pG* states predominantly follow paths 1 and 2, while in both Lbif PYP and the Ile68Pro mutant, the excited pG* states follow paths 1 and 3.

subpopulations results in generation of three kinetically distinct pG* populations that either initiate the photocycle via formation of the I_o intermediate (path 1), relax into a short-lived ground-state intermediate[23,36] (GSI) before evolving back into the pG populations (path 2), or skip the GSI and evolve directly into the original pG populations (path 3). We found (see below) that this model has sufficient flexibility to address the dynamics of all three samples studied here with the parameters listed in Table 1. The GSI populations could not be resolved for the Lbif PYP because of its slow excited-state dynamics, and we used a modified kinetic scheme to allow direct recovery to the ground state (Scheme 2, path 3).

The excited-state decay in Lbif PYP is triphasic with time constants of 0.2, 7, and 64 ps (Table 1 and Figure 3B). Similar triphasic excited-state decay kinetics have been detected in multiple studies of HhaI PYP[21−23,36] and are also observed in our analysis with time constants of 0.5, 2.7, and 21 ps. The structural inhomogeneity responsible for these three phases in HhaI PYP is still unresolved but is likely caused by small-scale conformational heterogeneity of the surrounding residues in the initial pG dark state of PYP. The primary difference between HhaI PYP and Lbif PYP is the relative amplitude of these three phases: in HhaI PYP, the fastest component (0.5 ps) contributes 50%, while in Lbif PYP, 50% of the population decays in the slowest 64 ps component.

In both WT and Ile68Pro Lbif PYP, proteins exhibit different decay kinetics of the SE signals (Figure 3C,E, red curves) and ESA signals (Figure 3C,E, blue curves). Because both of these signals originate from same pG* populations, and the "SE kinetics" are faster than the "ESA kinetics", these differences are interpreted as an overlapping transient photoproduct around 500 nm (Figure S7). This population is not clearly visible in the raw spectra because the slow decay of the negative SE signal overlaps its growth and decay kinetics (an inversion of time scales). Fortunately, global analysis is able to extract a SADS of this transient state (Figure 4B,C, green curve), which is assigned to a short-lived I_0 population. This spectrum peaks around 500 nm and appears between pG* and pR (Figure 4B,C, green curves). Because we could not resolve a GSI population in either Lbif PYP sample, it is possible that this spectrum represents the combination of the I_0 and GSI populations.

The terminal SADS resolved after decay of I_0 for both Lbif PYP samples exhibit positive signals at 360 nm (Figure 5). In transient absorption, positive signals can result from only ESA or photoproduct bands. Because no excited-state signals are present after 300 ps, this positive absorption cannot come from

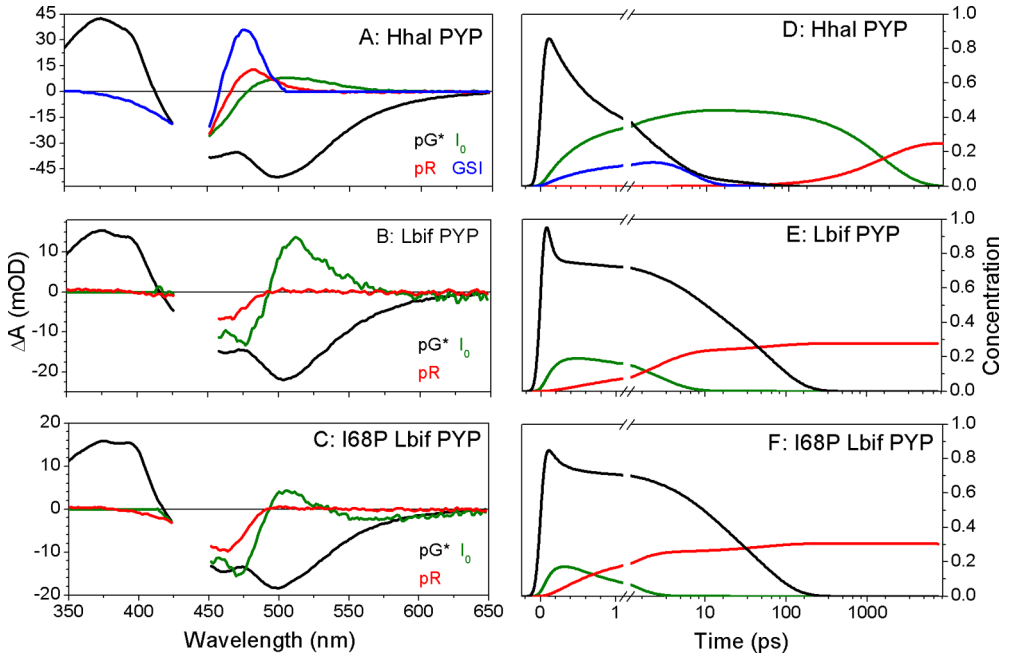

Figure 4. Species-associated difference spectra (SADS) and population kinetics for WT HhaI PYP, WT Lbif PYP, and Ile68Pro Lbif PYP. All three pG* excited-state intermediate (ESI) populations are merged into a single trace for the sake of readability. Spectra are color-coded by state for each protein.

DOI: 10.1021/acs.biochem.6b00547
Biochemistry XXXX, XXX, XXX−XXX

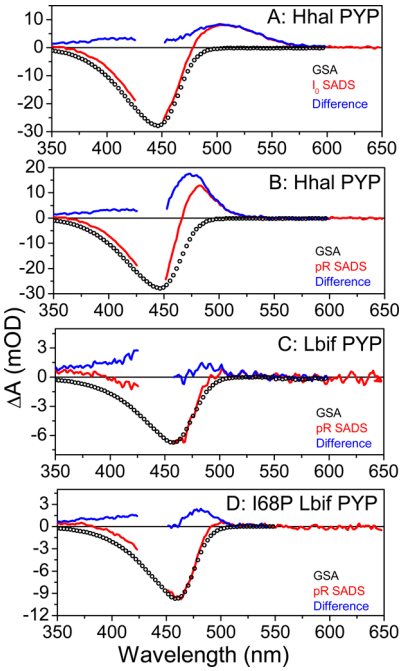

Figure 5. Comparison of photoproduct spectra with the inverted ground-state spectrum of each protein (○) for (A and B) WT Hhal PYP, (C) WT Lbif PYP, and (D) Ile68Pro Lbif PYP. Difference spectra have been reconstructed by subtracting the scaled inverted GSA from the terminal spectra (blue curves).

ESA and must be a photoproduct. Therefore, the final SADS states for Lbif PYP and Ile68Pro Lbif PYP appear to be mixtures of pR and a blue-shifted photoproduct. This is a novel observation, because such clear features of a blue-shifted photoproduct have not been reported before in ultrafast observations of PYP.

Cryokinetic Measurements. To shed more light on the possible occurrence of an early blue-shifted photoproduct, we developed a variant of cryotrapping experiments in which transient photoproducts are trapped at low temperatures. In the classical variant of this experiment, a light-sensitive protein is cooled to low temperatures and then exposed to visible light to generate the photoproduct. The sample temperature is then gradually increased, and the resulting spectral changes are recorded. In this approach, the general notion is that the lifetime of an intermediate at room temperature is related to the temperature at which it will thermally convert to the next photocycle intermediate. Intermediates with shorter lifetimes will proceed forward in the photocycle at a lower temperature due to the small barrier that needs to be overcome. In the experiments performed here, the cryotrapped species is exposed to a sudden temperature increase (a *T*-jump), and the kinetic changes in absorbance are recorded (albeit with a time resolution of minutes instead of 100 fs in the ultrafast TA measurements). The observed kinetics will be governed by the energy barrier separating the observed species; we refer to this approach as cryokinetic experiments.

To examine the occurrence of an early blue-shifted intermediate, we performed a series of cryokinetic measurements on Hhal PYP. The full data with 10 K *T*-jumps are depicted in Figures S2−S4 with select cyrokinetics at different *T*-jumps contrasted in Figure 6. The 80 K → 90 K *T*-jump signals (Figure 6A−C) exhibit a red-shifted state corresponding to I_0 in the ultrafast data along with hints of a UV-absorbing state that we call pUV. Spectra recorded over 1 h as the protein thermally equilibrates at 90 K show the absorbance of I_0 decreases as that of pUV increases, indicating a connection between the I_0 and pUV state. At higher temperatures in the 120 K → 130 K *T*-jump signals (Figure 6D−F), the pUV signals are well-resolved and I_0 has completely decayed. There are hints of the pR state as a positive signal persists at 475 nm, but it is not obvious because of the scattering background, which could not be removed completely. Above 160 K, the spectra are free of scatter as it is not cold enough for the glasslike protein sample to crack. In the 160 K → 170 K *T*-jump signals (Figure 6G−I), the well-resolved decay of pUV is accompanied by the growth of the pR state. The growth of pR and decay of pUV continue in the 170 K → 180 K cryokinetics (Figure 6J−L). The simultaneous changes in the pR and pUV states also indicate than equilibrium may exist between these two states. The pUV state is distinct from the pB[41] terminal signaling state of Hhal PYP, which is not observed in the cryokinetic experiment.[38] The 200 K → 210 K cryokinetics (Figure 6M−O) track the dark reversion from pR into pG without resolving the pB state.

DISCUSSION

The results reported here reveal both striking similarities and distinct differences between the highly studied Hhal PYP and the recently discovered Lbif PYP. Despite sharing only 38% amino acid sequence identity with Hhal PYP, the WT and Ile68Pro mutant Lbif PYPs exhibit nearly identical ESA and SE spectral characteristics with triphasic decay kinetics of pG* (albeit with slower kinetics). These results imply that the initial stages of the photocycle are conserved in members of the PYP family that exhibit fairly strong sequence divergence in the apoprotein. In addition, the data reported here for Lbif PYP indicate that triphasic excited-state decay is a general feature in the PYP family of photoreceptors.

In contrast to the spectral similarities of pG* between Hhal and Lbif PYP, the decay kinetics of the excited state in Lbif PYP are 10-fold slower, with Lbif PYP exhibiting the slowest excited-state decay of any known PYP protein or mutant to date. Sequence comparison of the residues in the chromophore pocket between Hhal and Lbif PYP suggests Ile68, Ala50, and Val52 as likely candidates for residues being responsible for the 10-fold slower decay of the excited state in Lbif PYP. Because the Ile68Pro mutation only slightly accelerates the excited-state decay in Lbif PYP, it is not a major contributor to the increased lifetime of the excited state in this photoreceptor. This is in agreement with the results of Groot et al., who determined that the excited-state decay kinetics and quantum yields are largely unchanged in the Pro68Val mutant of Hhal PYP.[21] Hhal PYP Glu46 mutants[46] that remove a hydrogen bond partner from *p*CA showed slower excited-state dynamics without a decrease in quantum yield. The Ala50 mutation in Lbif PYP similarly removes a hydrogen bond partner when compared to WT Hhal PYP but displays a slowing of the dynamics more pronounced than that observed in Glu46Ala Hhal PYP.[46] Ultrafast spectroscopic studies of Hhal PYP mutants by Changent-Barret et al.[23] revealed that the Thr50Val and Arg52Gln mutations slow excited-state decay in Hhal PYP by redistributing the heterogeneous populations into slower, less productive states. The triphasic decay kinetics in Lbif PYP is also a result of heterogeneous populations that favor the slower decaying excited state; 52% of the Lbif PYP sample decays with the slowest rate (64 ps) compared to only 6% in the slowest

DOI: 10.1021/acs.biochem.6b00547
Biochemistry XXXX, XXX, XXX−XXX

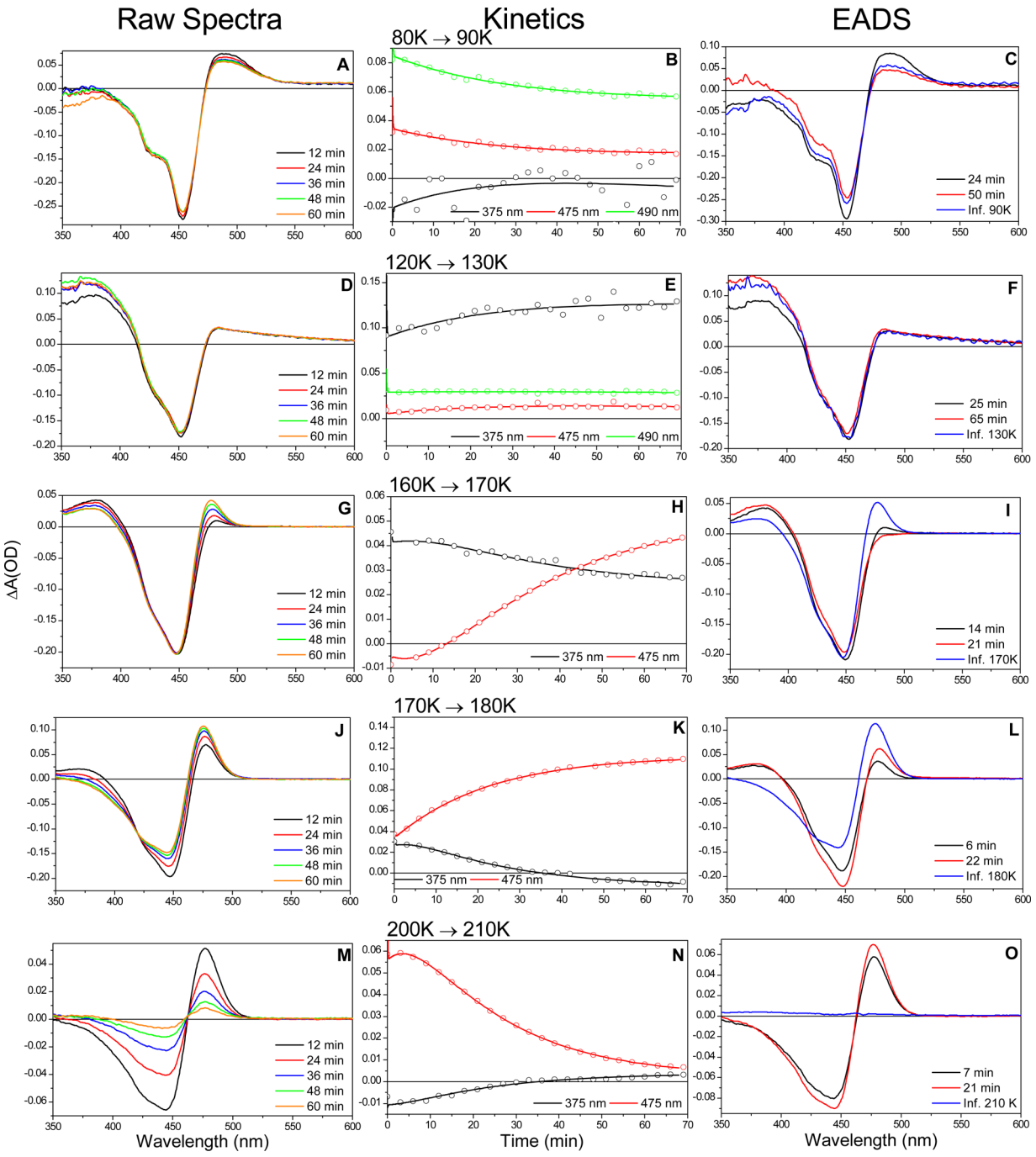

Figure 6. Cryokinetic raw spectra, kinetic traces, and sequential global analysis EADS of Hhal PYP. I_0 features a peak at 490 nm at 90 K, with weak pUV signals at 380 nm. At 130 K, I_0 has decayed and pUV continues to grow. At 170 and 180 K, pUV decays while pR grows in at 475 nm. The 210 K spectrum shows the dark reversion of pR into ground state pG, and the light state pB is not observed.

(45 ps) decaying excited Hhal PYP state. The combination of the naturally occurring residues Ala and Val at positions 50 and 52 in Lbif PYP significantly slows the excited-state decay, affecting the rate of the initial step of the PYP photocycle by decreasing the extent of hydrogen bonding between the *p*CA and protein and by redistributing its decay over the three available kinetic channels without decreasing the yield.

The photochemical quantum yields of Hhal PYP and both Lbif PYPs were calculated from the global analysis lifetimes listed in Table 1. It should be noted that yields, especially in inhomogeneous systems, are difficult to estimate; those estimated here have an associated relative error of 10% for Hhal PYP and 20% for Lbif PYP. The quantum yield for I_0 in Hhal PYP is 45% based on the GSB signals. Because the absorbance peak of the GSB signal decreases while its shape on the high-energy side (Figure S5) is maintained as Hhal PYP progresses from I_0 to the pR state (Figure 2) with the reasonable assumption that the I_0 and pR spectra are not equal in the bleach region, we concluded that the pG population is increasing. At this time in the photocycle, ~50 ps, all of the pG* has decayed and the increase in the ground-state population cannot originate from pG*. Therefore, some of the I_0 population fails to propagate to pR and returns to pG (perhaps via the GSI) to decrease the intensity of the GSB

DOI: 10.1021/acs.biochem.6b00547
Biochemistry XXXX, XXX, XXX−XXX

signal. Our global analysis estimates that 36% of the I_0 population decays into GSI and then pG, while 64% proceeds forward to generate pR. The effective pR yield of 29% reported here is in agreement with ultrafast visible pump−probe WT Hhal PYP studies,[36,47] although other studies[21,23,48] assumed a 100% conversion from I_0 to pR; i.e., the pG* to I_o step exclusively determines the photocycle yield.

The overall pR yields in Lbif PYP were surprisingly similar to those of Hhal PYP given the large difference in pR signal amplitude (Table 1) with a quantum yield of 27% for WT Lbif PYP and 30% for Ile68Pro Lbif PYP. Unlike in Hhal PYP, in Lbif PYP we did assume 100% of the I_0 population proceeded to pR. The inversion of time scales for evolution of I_o in the Lbif PYP samples made it impossible to estimate the I_0 to pR yield. If we were able to observe a GSI state in Lbif PYP, we would expect a similar behavior for the I_0 and GSI states as in Hhal PYP. The relatively large quantum yield for pR formation in Lbif PYP as compared to the small amplitude of the photoproduct signals in the ultrafast difference spectra can be explained by a small (15 nm) but significant red-shift of the peak of the GSB signal that hides the pR signal. The red-shift of the GSB in Lbif PYP compared to that in Hhal PYP is caused by the disruption of the hydrogen bond network with an Ala instead of Thr at position 50.[28,34] The spectral separation between the GSB and pR states is reduced to 15 nm in Lbif PYP from 30 nm in Hhal PYP, creating a situation in which the large negative GSB obscures the smaller positive pR signal. Subtracting the GSA inverted matched and scaled by eye to the GSB from the pR SADS reveals a significant pR amplitude for all three proteins, which peaks at 480 nm (Figure 5). Thus, the actual pR amplitude is larger than what appears in the SADS, particularly for Lbif PYP, in line with the derived quantum yield.

The Lbif PYP I68P mutant displays a slightly increased yield for pR of 30% over the 27% yield in the WT. This result agrees with experiments by Groot et al.[21] on photoproduct yields of Hhal PYP mutants at position 68. In Pro68Val, Pro68Ala, and Pro68Gly Hhal PYP, the residues with smaller side chains experienced the largest reductions in yield. As the Ile residue side chain is one carbon larger than Val, it is reasonable to observe only a small change in the yield for Ile68Pro Lbif PYP.

The final SADS of Lbif PYP (Figure 5) reveal a distinct signature for a blue-shifted photoproduct in the spectral region from 350 to 375 nm that clearly contains a positive absorption after the overlapping pG* spectrum had completely decayed. We believe this to be the same blue-shifted pUV photoproduct observed in the cryokinetic results at 130 K for Hhal PYP.

Further examination of the ultrafast SADS compared with the scaled inverted GSA signals in Figure 5 revealed that pUV signals are also present in Lbif PYP Ile68Pro and may also be weakly present in Hhal PYP. Interestingly, in the case of Ile68Pro Lbif PYP, the amplitude of the pR species is increased at the expense of the pUV band. Because Hhal PYP lacks a clearly defined bleach minimum in our data set, due to the pump pulse scattering, the inverted GSA could not be scaled exactly to the GSB. Therefore, the amplitude of the pUV absorption in Figure 5B for Hhal PYP is not quantitatively robust. A positive pUV band is also visible when the I_0 SADS are compared with the GSA (Figure 5A). However, from these observations combined with the cryokinetic data presented below for Hhal PYP, we are confident the blue-shifted pUV state does exist in WT Hhal PYP and both Lbif PYPs.

pUV is reminiscent of the properties of the Tyr42Phe[24] and Met100Glu[25] mutants of Hhal PYP, in which a fraction of the dark-state population absorbs at 390 nm that they called the intermediate spectral form.[24] Both Heyn and colleagues and Woolley and co-workers concluded that the blue-shifted intermediate spectral form contains a protonated *trans-p*CA chromophore.[24,25] The Tyr42Phe mutation[24] directly, and the Met100Glu mutation[25] indirectly, removes a hydrogen bond that stabilizes the deprotonated *p*CA phenolic hydroxyl group, strengthening the hydrogen bond from Glu46 to form *trans-p*CAH, yet the disruption of the hydrogen bonding network was not severe enough to disrupt the photocycle in the case of Met100Glu[25] or Tyr42Phe.[24] Heyn and Woolley introduced the possibility that an altered hydrogen bonding network could produce a blue-absorbing protonated *p*CA that is not the pB signaling state. Similarly in Lbif PYP (Scheme 1), the absence of the hydrogen bond between Thr50 and Tyr42 strengthens the Glu46 hydrogen bond and may promote the transfer of a proton to the *p*CA hydroxyl group. We propose that the pUV intermediate in Lbif PYP and Hhal PYP represents an early intermediate containing a protonated *p*CA chromophore because it has a spectral peak similar to that of the intermediate spectral form and a disruption of the hydrogen bonding network similar to those of the Tyr42Phe and Met100Glu mutations without abolishing the photocycle.

Cryokinetic experiments in our lab and cryotrapping measurements of Imamoto et al.[37,38] also argue for the existence of a blue photoproduct in Hhal PYP after formation of I_0 [PYP_B] and before pR [PYP_L]. Names for PYP photoproduct states from Imamoto are in brackets. Our cryokinetic experiments confirm the immediate formation of I_0 [PYP_B] at 80 K (Figure 6) but differ from those of Imamoto in that we do not detect a pUV [PYP_H] state immediately. The advantage of having kinetic data at low temperatures is that it allows us to observe pUV signals that develop over time as I_0 decays in the 80 K → 90 K *T*-jump. In these cryogenic experiments, we did not observe the pB state with an absorbance maximum 353 nm[41] compared to the pUV maximum at 390 nm. As the intensity of the pUV band increased, we observed a simultaneous decay in the I_0 signal, suggesting that the two states are in equilibrium. Subsequent analysis by illumination at the peak wavelengths of both states at low temperatures by Imamoto[38] indicated that I_0 [PYP_B] and pUV [PYP_H] decay into pR [PYP_L] above 190 K, evidence that pR and pUV are in equilibrium. Our cryokinetic traces show the decay of pUV and formation of pR from 160 to 180 K, in agreement with the results of Imamoto,[38] and add to the evidence for interconversion between pUV and pR. Ultrafast results from I68P Lbif PYP where the magnitude of the pR signal is increased at the expense of pUV (Figure 5C,D) validated the observed cryokinetic equilibria. Our cryokinetic data on Hhal PYP contribute to our understanding of the bifurcation proposed by Imamoto[37,38] of the PYP into red-shifted, pR [PYP_L] and blue-shifted, pUV [PYP_H] intermediate pathways. With the additional cryokinetic data, we propose that the pUV state is a protonated *p*CA chromophore with an unknown conformation that forms in equilibrium with the I_0 and pR states. However, we were not able to separate the bifurcation cleanly in the global analysis because of the weak pUV signal. The SADS shown for I_0 and pR (Figures 4 and 5) are linear combinations with pUV. If pUV is formed sequentially as observed in the cryokinetic and crystallography experiments (see below), I_0 and pUV and then pR and pUV

DOI: 10.1021/acs.biochem.6b00547
Biochemistry XXXX, XXX, XXX−XXX

Scheme 3. Revised Forward Photoreaction of PYP Proteins, Including the Unproductive Detour into the Protonated pUV State[a]

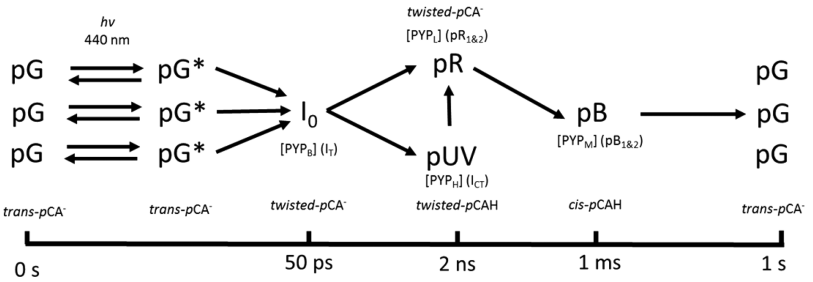

[a]The heterogeneous nature of the excited-state intermediate is shown by three separate pG and pG* states. The basic conformation of the *p*CA chromophore is labeled below or above each state. Alternate names for the states from Imamoto et al.[38] are shown in square brackets and those from Ihee and coworkers[35] in parentheses. Time scales are approximate; more detailed lifetimes are listed in Table 1.

will be present in the sample concurrently as the transformation propagates through the PYP population. This process leads to the presence of pUV signals in the I_0 and pR SADS.

The *p*CA conformations in the WT Hhal PYP and Glu46Gln mutant photocycle have been resolved nicely by Ihee and co-workers[19] via time-resolved X-ray crystallography. Names for photoproduct states from Ihee are given in parentheses. In WT Hhal PYP, they observed that the twisted *p*CA$^-$ I_0 (I_T) state could proceed to form the *cis*-*p*CA$^-$ pR state by a hula-twist motion or form a distinct state they called I_{CT} by a bicycle-pedal motion that subsequently forms *cis*-*p*CA$^-$ pR. Anfinrud and co-workers[49] dispute the bifurcation of the PYP crystallographic photocycle in favor of an equilibrium pathway.[50] However, bifurcation is also supported by low-temperature spectroscopy[37,38] and is supported by the ultrafast work reported here. In the Glu46Gln mutation,[19] I_{CT} was not present, and the bicycle-pedal motion and bifurcation of the photocycle did not occur. The crystallographic structure is not sufficient to observe hydrogen atoms. However, the removal of the hydrogen donor Glu46[17,24,25] quenches the formation of I_{CT}, implying that the hydrogen bond to the *p*CA may be important in stabilizing the I_{CT} structure and promoting branching. The Glu46 hydrogen bond is also crucial to formation of the proposed pUV state. We believe that the absence of I_{CT} in the Glu46Gln mutation along with its position in the photocycle between I_0 and pR, the same position where pUV is found in both ultrafast and cryokinetic measurements, indicates that the ultrafast pUV may have the same *p*CA structure as the I_{CT} state.

With the combined evidence from our ultrafast studies, mutation work,[24,25] cryokinetics and low-temperature difference spectra,[37,38] and crystallography,[35] we propose that the pUV state has a twisted *p*CAH chromophore that is a detour in the PYP photocycle. We have modified the photoreaction pathway from Ihee and co-workers[35] to include the ultrafast transient absorption data for PYP shown in Scheme 3. Alternate designations for the states from Imamoto and co-workers[37,38] are in square brackets and those from Ihee and co-workers[35] in parentheses. The heterogeneous dark state, pG, with the deprotonated *trans*-*p*CA$^-$ chromophore absorbs 445 nm light undergoing a transition to the excited pG* state. pG* decays in a triphasic[21,23,40] heterogeneous fashion with some of the population progressing to the twisted deprotonated I_0 *p*CA state within picoseconds. The twisted *p*CA$^-$ may be protonated, forming pUV, or continue forward to the *cis*-*p*CA$^-$ pR state. Any population that detours to the pUV state must release the proton and form pR to rejoin the pathway to the pB signaling state. The time scale of pUV formation and the transition into pR in Lbif PYP was not observed in the ultrafast experiments but must be longer than 7.5 ns as pUV signals are still present in the last recorded spectrum. Subsequently, the pR state is protonated in microseconds, and the protein undergoes large structural changes to form pB in milliseconds. The protonated *cis*-*p*CAH pB state is the biologically active signal state of the protein. Without further illumination, the pB state thermally reverts back into the pG ground state after ∼1 s and is ready to begin the signaling process again.

CONCLUDING COMMENTS

The mechanisms that allow photoreceptor proteins to greatly increase the quantum yield for chromophore alkene photoisomerization are not well understood. We examine a novel homologue of photoactive yellow protein (PYP) from *L. biflexa* to identify conserved features and functional diversity in the primary photochemistry of this family of photoreceptors. In close agreement with the prototypical PYP from *H. halophila*, we observe excited-state absorbance near 375 nm and stimulated emission near 500 nm, with triphasic excited-state decay. The excited-state decay for Lbif PYP is the slowest yet observed in any PYP because the majority of the heterogeneous ground-state population occupies slower, less productive states. While Pro68 is highly conserved in PYPs and is important for the high photochemical quantum yield of Hhal PYP, this residue is Ile in wild-type Lbif PYP. The Ile68Pro mutation causes a small increase in the level of photoproduct formation in Lbif PYP, indicating that this residue regulates the photochemical quantum yield in the entire PYP family. Lbif PYP also exhibited signs of a blue-shifted photoproduct previously undiscovered in any ultrafast transient absorption study of PYP that we named pUV. pUV is also present in ultrafast and cryokinetic Hhal PYP spectra. We posit that pUV is a twisted protonated form of *p*CA that creates a detour in the photoreaction of PYP proteins. Our data resolve the inconsistency in the current PYP literature in which some groups describe the early stages of the PYP photocycle as bifurcating whereas others do not. We find clear evidence of an early blue-shifted species in cryokinetic measurements of Hhal PYP and room-temperature ultrafast pump−probe measurements of Lbif PYP. However, the amplitude of this blue-shifted species is very small in Hhal PYP, explaining why it has not been reported in previous ultrafast experiments with this PYP.

DOI: 10.1021/acs.biochem.6b00547
Biochemistry XXXX, XXX, XXX−XXX

■ ASSOCIATED CONTENT

Supporting Information

The Supporting Information is available free of charge on the ACS Publications website at DOI: 10.1021/acs.biochem.6b00547.

DNA primer sequences, experimental setup diagrams, and additional figures (PDF)

■ AUTHOR INFORMATION

Corresponding Author

*E-mail: dlarsen@ucdavis.edu.

Funding

This work was supported by a grant from the National Science Foundation (NSF) (CHE-1413739) to both D.S.L. and W.D.H. W.D.H. acknowledges additional support from NSF Grants MCB-1051590 and MRI-1338097.

Notes

The authors declare no competing financial interest.

■ ABBREVIATIONS

PYP, photoactive yellow protein; Lbif, *L. biflexa*; Hhal, *H. halophila*; WT, wild type; *p*CA, *p*-coumaric acid; fwhm, full width at half-maximum; NOPA, nonlinear optical parametric amplifier; TA, transient absorption; S/N, signal to noise; GSB, ground-state bleach; ESA, excited-state absorptions; SE, stimulated emission; GSI, ground-state intermediate; EADS, evolution-associated difference spectrum; SADS, species-associated difference spectrum.

■ REFERENCES

(1) Bhaya, D. (2004) Light matters: phototaxis and signal transduction in unicellular cyanobacteria. *Mol. Microbiol. 53*, 745−754.

(2) Sprenger, W. W., Hoff, W. D., Armitage, J. P., and Hellingwerf, K. J. (1993) The eubacterium Ectothiorhodospira halophila is negatively phototactic, with a wavelength dependence that fits the absorption spectrum of the photoactive yellow protein. *J. Bacteriol. 175*, 3096−3104.

(3) Quail, P. H. (1991) Phytochrome: a light-activated molecular switch that regulates plant gene expression. *Annu. Rev. Genet. 25*, 389−409.

(4) Briggs, W. R., and Spudich, J. L., Eds. (2005) *Handbook of Photosensory Receptors*, Wiley-VCH, Weinheim, Germany.

(5) Baylor, D. (1996) How photons start vision. *Proc. Natl. Acad. Sci. U. S. A. 93*, 560−565.

(6) Kehoe, D. M., and Grossman, A. R. (1994) Complementary chromatic adaptation: photoperception to gene regulation. *Semin. Cell Biol. 5*, 303−313.

(7) Whitmarsh, J., and Govindjee (1995) Photosynthesis. In *Encyclopedia of Applied Physics*, pp 513−532, VCH Publishers Inc., Weinheim, Germany.

(8) Béjà, O., Pinhassi, J., and Spudich, J. L. (2013) Proteorhodopsins: Widespread Microbial Light-Driven Proton Pumps. In *Encyclopedia of Biodiversity* (Levin, S. A., Ed.) 2nd ed., pp 280−285, Academic Press, Waltham, MA.

(9) Moser, C. C., Keske, J. M., Warncke, K., Farid, R. S., and Dutton, P. L. (1992) Nature of biological electron transfer. *Nature 355*, 796−802.

(10) Kukura, P., McCamant, D. W., Yoon, S., Wandschneider, D. B., and Mathies, R. A. (2005) Structural Observation of the Primary Isomerization in Vision with Femtosecond-Stimulated Raman. *Science 310*, 1006−1009.

(11) Mataga, N., Chosrowjan, H., Shibata, Y., Imamoto, Y., and Tokunaga, F. (2000) Effects of Modification of Protein Nanospace Structure and Change of Temperature on the Femtosecond to Picosecond Fluorescence Dynamics of Photoactive Yellow Protein. *J. Phys. Chem. B 104*, 5191−5199.

(12) Deisseroth, K. (2011) Optogenetics. *Nat. Methods 8*, 26−29.

(13) Müller, K., and Weber, W. (2013) Optogenetic tools for mammalian systems. *Mol. BioSyst. 9*, 596−608.

(14) Hoff, W. D., Dux, P., Hard, K., Devreese, B., Nugteren-Roodzant, I. M., Crielaard, W., Boelens, R., Kaptein, R., Van Beeumen, J., and Hellingwerf, K. J. (1994) Thiol ester-linked p-coumaric acid as a new photoactive prosthetic group in a protein with rhodopsin-like photochemistry. *Biochemistry 33*, 13959−13962.

(15) Groot, M. L., van Wilderen, L. J. G. W., Larsen, D. S., van der Horst, M. A., van Stokkum, I. H. M., Hellingwerf, K. J., and van Grondelle, R. (2003) Initial Steps of Signal Generation in Photoactive Yellow Protein Revealed with Femtosecond Mid-Infrared Spectroscopy†. *Biochemistry 42*, 10054−10059.

(16) Heyne, K., Mohammed, O. F., Usman, A., Dreyer, J., Nibbering, E. T. J., and Cusanovich, M. A. (2005) Structural Evolution of the Chromophore in the Primary Stages of Trans/Cis Isomerization in Photoactive Yellow Protein. *J. Am. Chem. Soc. 127*, 18100−18106.

(17) Xie, A., Hoff, W. D., Kroon, A. R., and Hellingwerf, K. J. (1996) Glu46 Donates a Proton to the 4-Hydroxycinnamate Anion Chromophore During the Photocycle of Photoactive Yellow Protein. *Biochemistry 35*, 14671−14678.

(18) Xie, A., Kelemen, L., Hendriks, J., White, B. J., Hellingwerf, K. J., and Hoff, W. D. (2001) Formation of a New Buried Charge Drives a Large-Amplitude Protein Quake in Photoreceptor Activation†. *Biochemistry 40*, 1510−1517.

(19) Ihee, H., Rajagopal, S., Šrajer, V., Pahl, R., Anderson, S., Schmidt, M., Schotte, F., Anfinrud, P. A., Wulff, M., and Moffat, K. (2005) Visualizing reaction pathways in photoactive yellow protein from nanoseconds to seconds. *Proc. Natl. Acad. Sci. U. S. A. 102*, 7145−7150.

(20) Meyer, T. E. (1985) Isolation and characterization of soluble cytochromes, ferredoxins and other chromophoric proteins from the halophilic phototrophic bacterium Ectothiorhodospira halophila. *Biochim. Biophys. Acta, Bioenerg. 806*, 175−183.

(21) Rupenyan, A. B., Vreede, J., van Stokkum, I. H. M., Hospes, M., Kennis, J. T. M., Hellingwerf, K. J., and Groot, M. L. (2011) Proline 68 Enhances Photoisomerization Yield in Photoactive Yellow Protein. *J. Phys. Chem. B 115*, 6668−6677.

(22) Changenet-Barret, P., Plaza, P., Martin, M. M., Chosrowjan, H., Taniguchi, S., Mataga, N., Imamoto, Y., and Kataoka, M. (2007) Role of arginine 52 on the primary photoinduced events in the PYP photocycle. *Chem. Phys. Lett. 434*, 320−325.

(23) Changenet-Barret, P., Plaza, P., Martin, M. M., Chosrowjan, H., Taniguchi, S., Mataga, N., Imamoto, Y., and Kataoka, M. (2009) Structural Effects on the Ultrafast Photoisomerization of Photoactive Yellow Protein. Transient Absorption Spectroscopy of Two Point Mutants†. *J. Phys. Chem. C 113*, 11605−11613.

(24) Joshi, C. P., Otto, H., Hoersch, D., Meyer, T. E., Cusanovich, M. A., and Heyn, M. P. (2009) Strong Hydrogen Bond between Glutamic Acid 46 and Chromophore Leads to the Intermediate Spectral Form and Excited State Proton Transfer in the Y42F Mutant of the Photoreceptor Photoactive Yellow Protein. *Biochemistry 48*, 9980−9993.

(25) Kumar, A., and Woolley, G. A. (2015) Origins of the Intermediate Spectral Form in M100 Mutants of Photoactive Yellow Protein. *Photochem. Photobiol. 91*, 985−991.

(26) Kroon, A. R., Hoff, W. D., Fennema, H. P. M., Gijzen, J., Koomen, G.-J., Verhoeven, J. W., Crielaard, W., and Hellingwerf, K. J. (1996) Spectral Tuning, Fluorescence, and Photoactivity in Hybrids of Photoactive Yellow Protein, Reconstituted with Native or Modified Chromophores. *J. Biol. Chem. 271*, 31949−31956.

(27) Meyer, T. E., Kyndt, J. A., Memmi, S., Moser, T., Colon-Acevedo, B., Devreese, B., and Van Beeumen, J. J. (2012) The growing family of photoactive yellow proteins and their presumed functional roles. *Photochemical & Photobiological Sciences 11*, 1495−1514.

(28) Kumauchi, M., Hara, M. T., Stalcup, P., Xie, A., and Hoff, W. D. (2008) Identification of Six New Photoactive Yellow Proteins—

DOI: 10.1021/acs.biochem.6b00547
Biochemistry XXXX, XXX, XXX−XXX

Diversity and Structure−Function Relationships in a Bacterial Blue Light Photoreceptor†. *Photochem. Photobiol. 84*, 956−969.
(29) Harigai, M., Yasuda, S., Imamoto, Y., Yoshihara, K., Tokunaga, F., and Kataoka, M. (2001) Amino Acids in the N-Terminal Region Regulate the Photocycle of Photoactive Yellow Protein. *J. Biochem. 130*, 51−56.
(30) Groenhof, G., Bouxin-Cademartory, M., Hess, B., de Visser, S. P., Berendsen, H. J. C., Olivucci, M., Mark, A. E., and Robb, M. A. (2004) Photoactivation of the Photoactive Yellow Protein: Why Photon Absorption Triggers a Trans-to-Cis Isomerization of the Chromophore in the Protein. *J. Am. Chem. Soc. 126*, 4228−4233.
(31) Groenhof, G., Schäfer, L. V., Boggio-Pasqua, M., Grubmüller, H., and Robb, M. A. (2008) Arginine52 Controls the Photoisomerization Process in Photoactive Yellow Protein. *J. Am. Chem. Soc. 130*, 3250−3251.
(32) Yamaguchi, S., Kamikubo, H., Kurihara, K., Kuroki, R., Niimura, N., Shimizu, N., Yamazaki, Y., and Kataoka, M. (2009) Low-barrier hydrogen bond in photoactive yellow protein. *Proc. Natl. Acad. Sci. U. S. A. 106*, 440−444.
(33) Stahl, A. D., Hospes, M., Singhal, K., van Stokkum, I., van Grondelle, R., Groot, M. L., and Hellingwerf, K. J. (2011) On the Involvement of Single-Bond Rotation in the Primary Photochemistry of Photoactive Yellow Protein. *Biophys. J. 101*, 1184−1192.
(34) Mataga, N., Chosrowjan, H., Shibata, Y., Imamoto, Y., Kataoka, M., and Tokunaga, F. (2002) Ultrafast photoinduced reaction dynamics of photoactive yellow protein (PYP): observation of coherent oscillations in the femtosecond fluorescence decay dynamics. *Chem. Phys. Lett. 352*, 220−225.
(35) Jung, Y. O., Lee, J. H., Kim, J., Schmidt, M., Moffat, K., Šrajer, V., and Ihee, H. (2013) Volume-conserving trans-cis isomerization pathways in photoactive yellow protein visualized by picosecond X-ray crystallography. *Nat. Chem. 5*, 212−220.
(36) Larsen, D. S., van Stokkum, I. H. M., Vengris, M., van der Horst, M. A., de Weerd, F. L., Hellingwerf, K. J., and van Grondelle, R. (2004) Incoherent Manipulation of the Photoactive Yellow Protein Photocycle with Dispersed Pump-Dump-Probe Spectroscopy. *Biophys. J. 87*, 1858−1872.
(37) Imamoto, Y., Shirahige, Y., Tokunaga, F., Kinoshita, T., Yoshihara, K., and Kataoka, M. (2001) Low-Temperature Fourier Transform Infrared Spectroscopy of Photoactive Yellow Protein. *Biochemistry 40*, 8997−9004.
(38) Imamoto, Y., Kataoka, M., and Tokunaga, F. (1996) Photoreaction Cycle of Photoactive Yellow Protein from Ectothiorhodospira halophila Studied by Low-Temperature Spectroscopy. *Biochemistry 35*, 14047−14053.
(39) Mihara, K. i., Hisatomi, O., Imamoto, Y., Kataoka, M., and Tokunaga, F. (1997) Functional Expression and Site-Directed Mutagenesis of Photoactive Yellow Protein. *J. Biochem. 121*, 876−880.
(40) Larsen, D. S., Vengris, M., van Stokkum, I. H. M., van der Horst, M. A., de Weerd, F. L., Hellingwerf, K. J., and van Grondelle, R. (2004) Photoisomerization and Photoionization of the Photoactive Yellow Protein Chromophore in Solution. *Biophys. J. 86*, 2538−2550.
(41) Carroll, E. C., Song, S.-H., Kumauchi, M., van Stokkum, I. H. M., Jailaubekov, A., Hoff, W. D., and Larsen, D. S. (2010) Subpicosecond Excited-State Proton Transfer Preceding Isomerization During the Photorecovery of Photoactive Yellow Protein. *J. Phys. Chem. Lett. 1*, 2793−2799.
(42) Ujj, L., Devanathan, S., Meyer, T. E., Cusanovich, M. A., Tollin, G., and Atkinson, G. H. (1998) New Photocycle Intermediates in the Photoactive Yellow Protein from Ectothiorhodospira halophila: Picosecond Transient Absorption Spectroscopy. *Biophys. J. 75*, 406−412.
(43) Joshi, C. P., Borucki, B., Otto, H., Meyer, T. E., Cusanovich, M. A., and Heyn, M. P. (2005) Photoreversal Kinetics of the I1 and I2 Intermediates in the Photocycle of Photoactive Yellow Protein by Double Flash Experiments with Variable Time Delay. *Biochemistry 44*, 656−665.
(44) van Stokkum, I. H. M., Larsen, D. S., and van Grondelle, R. (2004) Global and target analysis of time-resolved spectra. *Biochim. Biophys. Acta, Bioenerg. 1657*, 82−104.
(45) Holzwarth, A. (1996) Data Analysis of Time-Resolved Measurements. In *Biophysical Techniques in Photosynthesis* (Amesz, J., and Hoff, A., Eds.) pp 75−92, Springer, Dordrecht, The Netherlands.
(46) Zhu, J., Vreede, J., Hospes, M., Arents, J., Kennis, J. T. M., van Stokkum, I. H. M., Hellingwerf, K. J., and Groot, M. L. (2015) Short Hydrogen Bonds and Negative Charge in Photoactive Yellow Protein Promote Fast Isomerization but not High Quantum Yield. *J. Phys. Chem. B 119*, 2372−2383.
(47) van Brederode, M. E., Gensch, T., Hoff, W. D., Hellingwerf, K. J., and Braslavsky, S. E. (1995) Photoinduced volume change and energy storage associated with the early transformations of the photoactive yellow protein from Ectothiorhodospira halophila. *Biophys. J. 68*, 1101−1109.
(48) van Wilderen, L. J. G. W., van der Horst, M. A., van Stokkum, I. H. M., Hellingwerf, K. J., van Grondelle, R., and Groot, M. L. (2006) Ultrafast infrared spectroscopy reveals a key step for successful entry into the photocycle for photoactive yellow protein. *Proc. Natl. Acad. Sci. U. S. A. 103*, 15050−15055.
(49) Kaila, V. R. I., Schotte, F., Cho, H. S., Hummer, G., and Anfinrud, P. A. (2014) Contradictions in X-ray structures of intermediates in the photocycle of photoactive yellow protein. *Nat. Chem. 6*, 258−259.
(50) Schotte, F., Cho, H. S., Kaila, V. R. I., Kamikubo, H., Dashdorj, N., Henry, E. R., Graber, T. J., Henning, R., Wulff, M., Hummer, G., Kataoka, M., and Anfinrud, P. A. (2012) Watching a signaling protein function in real time via 100-ps time-resolved Laue crystallography. *Proc. Natl. Acad. Sci. U. S. A. 109*, 19256−19261.

DOI: 10.1021/acs.biochem.6b00547
Biochemistry XXXX, XXX, XXX−XXX